IMPROVING DISCRIMINANTS FOR SOURCE IDENTIFICATION

Thorne Lay and Guangwei Fan

University of California, Santa Cruz

Sponsored by Defense Threat Reduction Agency

Contract No. DTRA01-00-C-0211

ABSTRACT

The ability to correct regional phase discriminant measurements for propagation effects is strongly influenced by the nature of the propagation phenomenon. As an example, blockage of Lg phases by waveguide disruption may lead to enhanced Sn amplitudes, allowing effective discrimination to proceed by interchanging P/Sn ratios for P/Lg ratios, or the corresponding use of Smax measurements. However, if the Lg phase is strongly damped out by intrinsic attenuation, there will be no compensating flux of energy into the Sn wavefield (or vice versa). In addition, the theoretical nature of corrections for amplitude loss for regional phases is expected to assume distinct functional forms for attenuation versus scattering phenomena, and interpolation and extrapolation of empirical corrections should differ for diverse propagation phenomena. The research project that we are pursuing involves exploration of hybrid methods of kriging, parametric regression analysis, and modeling to develop optimal capabilities for correcting for propagation effects. The overriding challenge within central Asia appears to be how to account for, or at least recognize, strong losses of Lg amplitudes for propagation paths within the Tibetan Plateau. Motivated by earlier results from other groups which reported relatively moderate attenuation values for Lg phases within and traversing the Plateau, we assembled a large database which persuasively demonstrated to us that Lg amplitude decay was more rapid than predicted by published attenuation models. One possible cause was a blockage effect associated with loss of Lg energy upon crossing the Plateau margins, but our analysis suggested that the data are more consistent with progressive energy losses proportional to path length within the Plateau, only at a much more severe rate of attenuation than published work would lead us to expect. We developed a differential spectral approach using multiple events with common paths outside of the Plateau but different path lengths in the Plateau to robustly estimate broadband Lg spectral decay. Rather phenomenal evolution of the Lg spectra with path length is observed, with a strong systematic shift of the Lg 'corner' frequency from 2 Hz to 0.2 Hz as a function of increasing path length in the Plateau. Spectral ratios for various path geometries across Tibet indicate that attenuation values for 1-Hz Lg are on the order of 80-90 in the northern central area of Tibet where strong Sn attenuation has previously been mapped, and on the order of 130-150 in most other areas of Tibet. These values are as much as 3 to 4 times lower than published values, but are consistent with (and derived from) the observed progressive extinction of broadband Lg energy. Reanalysis of earlier attenuation estimates has recently been conducted by J. Xie, and he also reports much lower Lg attenuation values within Tibet, consistent with our own estimates. The conclusion is that so-called blockage of Lg energy for paths in Tibet is in fact due to very strong crustal attenuation, of a magnitude likely to be linked to the presence of partial melt in the lower crust (as has been invoked for the upper mantle to account for Sn attenuation). Thus, there is no compensating transfer of energy from Lg to Sn via scattering that would enable a robust Smax solution to the discrimination problem for Tibet events. The observed internal heterogeneity of attenuation within the Plateau makes it difficult to develop alternate lower frequency Lg amplitude measures that might reflect source type as well. Reliance on alternate discriminant measures for Tibetan events appears mandatory.

KEY WORDS: seismic discriminants, regional seismic phases, amplitude corrections, regional wave propagation

OBJECTIVE

We seek to understand the absence of high-frequency *Lg* arrivals for paths traversing the northern boundary of the Tibetan Plateau. The regional signals for events within the Plateau recorded at stations outside the Plateau often appear rather explosion-like due to the weak *Sn* and *Lg* arrivals. Ruzaikin et al. (1977) found that a path length of 200 km within the Plateau is sufficient to attenuate 1-Hz *Lg* signals down to noise levels for observing stations located north of the Plateau. Those authors suggested that either strong attenuation or scattering by a thinning crustal waveguide was responsible, but they stated that their narrowband data did not resolve a progressive shift of *Lg* spectral content to lower frequencies with increasing path length in Tibet, as would be expected if attenuation is primarily responsible. They did note that very low Q values of 20-40 would be required to attenuate 1 Hz *Lg* energy by a factor of 100 over 100- to 200-km path lengths, as observed. Qualitative analysis of *Lg* propagation efficiency relative to *P*-wave coda for stations west and south of Tibet indicated that *Lg* signals are strongly attenuated within central and northern Tibet while the phase does propagate along the Himalayan mountain belt (Ni and Barazangi, 1983). This inefficient *Lg* propagation was again attributed to either strong crustal attenuation within Tibet or to waveguide disruption on the southern margin. Rapine et al. (1997) found inefficient *Lg* propagation across most of Tibet, with no *Lg* from western Himalayan events reaching either station WMQ to the north of the Tarim Basin or station LSA within Tibet (LSA did record *Lg* on some paths from events in the eastern Himalayas and eastern Tibet, suggesting internal variations in propagation efficiency within the Plateau).

McNamara et al. (1996) analyzed data recorded at 11 broadband stations in eastern central Tibet, finding that high frequency *Lg* is generated by events within the Plateau, and can propagate to distances of at least 600 km; however, the phase was not observed for paths traversing western or central Tibet or for events in the Himalayas. For eastern Tibet, where sufficient *Lg* signal to noise ratios were observed, a frequency-dependent Q function given by $Q(f) = (366–37)f^{(0.45–0.06)}$ was estimated for the passband (0.5-16 Hz) (McNamara et al., 1996). This is comparable to the estimate of $Q(f)=(448–82)f^{(0.426–0.157)}$ estimated for 1-6 s *Lg* waves traversing Tibet by Shih et al. (1994). This latter value is likely also dominated by eastern Tibet paths, as 'blocked' observations were omitted from the calculation. Similar Q_{Lg} value was also estimated to be 340 for events north of LSA using spectral methods by assuming a constant Q_{Lg} model (Reese et al., 1999). These attenuation values are typical of tectonically active areas, and are not low enough to cause rapid extinction of 1 Hz *Lg* over just a few hundred kilometers, as observed for paths traversing the northern margin of Tibet. One could then infer that waveguide disruption must cause extinction of *Lg* in the latter regions; however, this is not a secure interpretation because Q_{Lg} may vary laterally within Tibet. Indeed one might expect this to be the case, for it is true of *Sn* attenuation, which is strongest in northern central Tibet. The possibility of stronger *Lg* attenuation in northern and central Tibet is suggested by the lack of high frequency *Lg* detections for events to the west of the broadband stations in the data set of McNamara et al. (1996).

Our presentation resolves this issue, demonstrating the presence of very strong attenuation in the region of north-central Tibet, an area where other work has demonstrated the presence of partial melt in the crust. We also find average *QLg* values for the Plateau of about 150, much lower than proposed in earlier work.

RESEARCH ACCOMPLISHED

Our main data are regional waveforms recorded at broadband station WMQ, the westernmost station of the Chinese Digital Seismic Network. This station lies just north of the Tarim Basin, about 650 km from the northern boundary of the Tibetan Plateau (Figure 1). While three-component data were obtained, we restrict our analysis to the vertical component seismograms due to the attenuated nature of the *Lg* phases traversing Tibet, which leads to confusion with fundamental mode Love wave energy on the transverse components. We examine energy in the standard *Lg* group velocity window of 3.6 to 3.0 km/s, which precedes short and intermediate period fundamental mode Rayleigh wave energy. We analyze recordings for 90 earthquakes with magnitudes of $4.4 \le m_b \le 6.4$ that occurred between 1987 and 1999 in the Tibetan Plateau and around its margins. A few events with paths well removed from Tibet (Figure 1) were also analyzed.

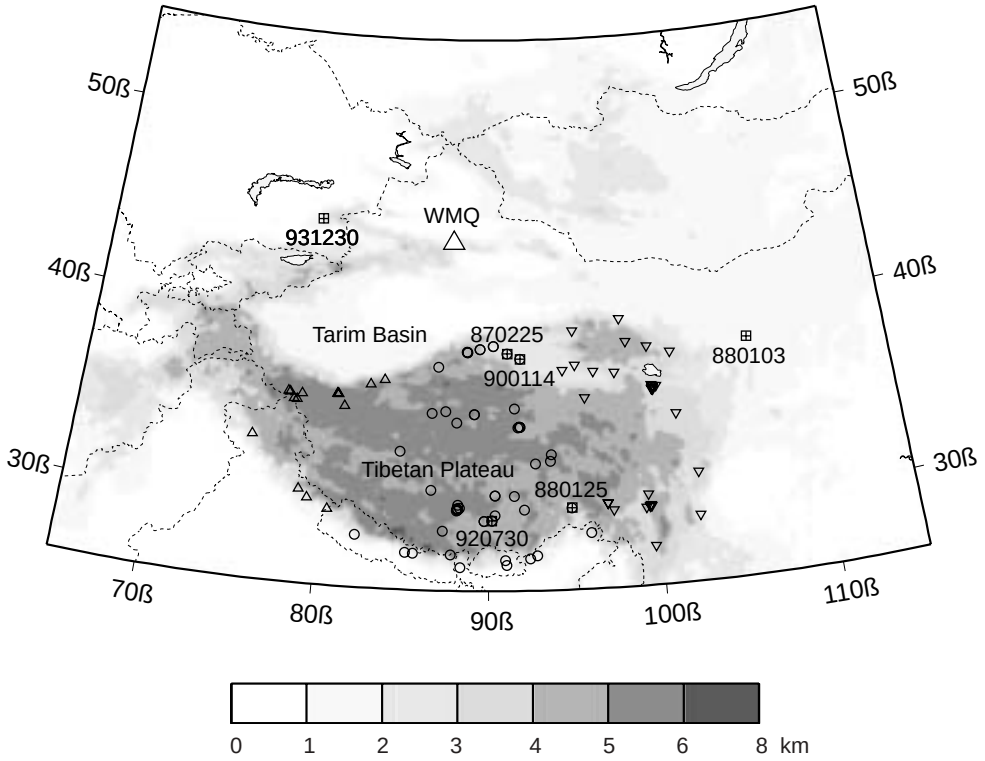

Figure 1. Topography in Western China and its vicinity. The location of station WMQ is shown. The squares, circles, triangles, and inverted triangles indicate the epicenters of the events for which spectra are shown. The events within Tibet are grouped into eastern (inverted triangles), central (circles) and western (triangles) groups.

The recorded seismograms show great variability in broadband waveforms, and our analysis is constrained to qualitative relative measures because we use only one station and cannot fully account for source effects. For events prior to 1998 the source parameters are taken from the International Seismological Centre (ISC) bulletin. For more recent events the source parameters are from the USGS Preliminary Determination of Epicenters (PDE) catalog. Only events with catalog focal depths less than 50 km are included. While catalog source depths in this region are subject to tens of kilometers of uncertainty, this criterion probably ensures that all events analyzed are crustal events, given that the crustal thickness in the central Tibetan Plateau is about 65 to 75 km. All selected events have signal-to-noise ratios greater than 2 for broadband measurements of the *Pn* signal and pre-*Pn* noise.

Figure 2 demonstrates the predominant feature of high frequency *Lg* propagation across the northern Tibetan Plateau boundary first documented by Ruzaikin et al. (1977). The records shown are for a roughly northwest to southeast profile of events, with the signals filtered in the bandpass 1.0-5.0 Hz. The first three records are for events located near the 4000 m topographic contour along the northern boundary of the Plateau. These show typical earthquake-like high frequency signals, with predominant *Lg* energy that is much stronger than the *Pn* arrivals. The lower two records are from events 250-400 km further to the southeast, and the maximum relative amplitude ratio of *Lg* to *P* energy is about a factor of ten lower than for the northwestern events, giving these signals explosion-like character. The distribution of events in Tibet (Figure 1) presents a challenge in that there is not a continuous distribution of events from the Plateau margin to the interior; this makes it difficult to separate possible waveguide disruption effects from strong crustal attenuation effects as causes for the high frequency *Lg* energy blockage. However; we can consider behavior of *Lg* at lower frequency on longer profiles to assess the role of attenuation in the Plateau, as this should be manifested in a progressive shift of the frequency content of *Lg* with propagation length across the Plateau as suggested by Molnar (Ruzaikin et al., 1977).

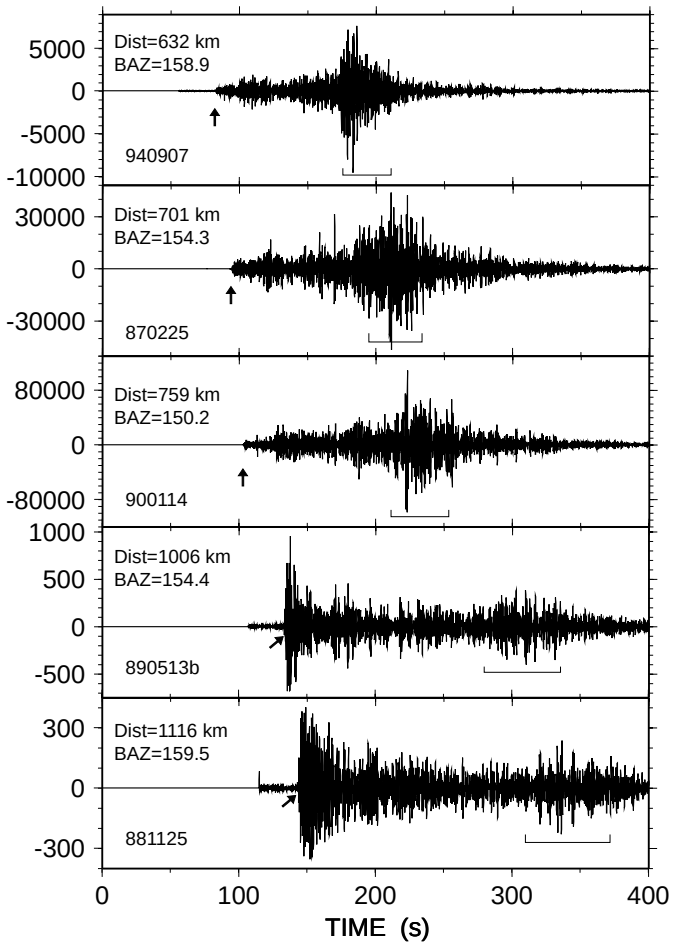

Figure 2. Demonstration of the rapid decrease of Lg energy near the northern Tibetan Plateau boundary. WMQ records are shown for a short NW-SE profile of events, with bandpass filters isolating the 1.0-5.0 Hz passband, for events near the northern boundary (top 3 records) and a few hundred kilometers into the Plateau (lower 2 records). The Lg group velocity window is indicated by the bracket below each seismogram. Small arrows represent the Pn arrivals after the onset of visible signal in each trace. There is about a factor of 10 decrease in the Lg/Pn amplitude ratio common to all events several hundred kilometers south of the Plateau boundary.

Figure 3 shows a longer profile of records, retaining the full broadband energy with amplitudes normalized relative to the 20 s Rayleigh wave energy in each signal. The dramatic shift of frequency content in the *Lg* group velocity window over the first few hundred kilometers is again apparent, but now it is apparent that there is also a progressive shift of frequency content and decrease of relative amplitudes in the *Lg* window for lower frequencies as path length across the Plateau increases.

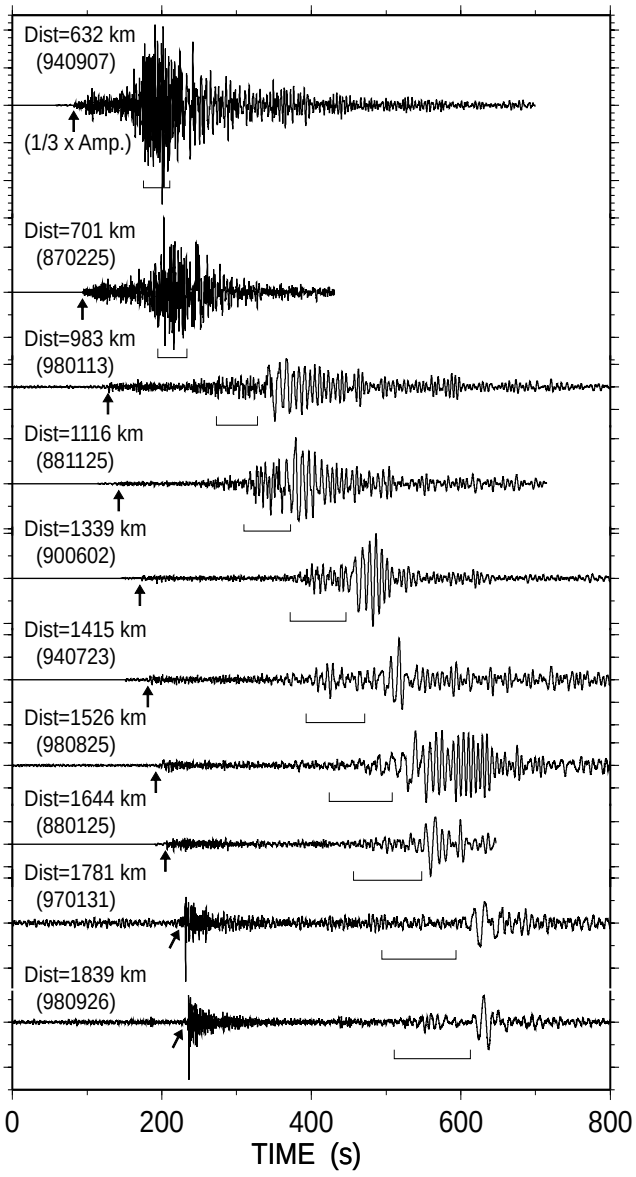

Figure 3. Broadband recordings at WMQ for events traversing the entire central portion of the Plateau. Each record has been amplitude-normalized relative to the 20 s Rayleigh wave energy.

We lack detailed knowledge of the source process and radiation effects for our events, and the station coverage is not adequate to enable empirical separation of source and propagation effects. However, our broadband digital data indicate that propagation effects dominate in shaping the *Lg* window.

Determination of *Lg* Attenuation

Our observations of *Lg* spectral content shifting to lower frequency with increased path length in Tibet demonstrate a strong, progressive *Lg* attenuation in the crust beneath the Plateau. Using a modified two-event method, we estimate *Lg* attenuation coefficient $\gamma(f)$ for the paths crossing several sectors of Tibet. Some constraints are placed on regional heterogeneity of *Lg* attenuation. The displacement spectral amplitude of the *Lg* wave arriving from a source at a distance *d* can be expressed in the form

$$A(f, d) = S(f)R(f, q)G(d)G(f, q)I(f)SS(f), \quad (1)$$

where *f* denotes the frequency, *q* the station azimuth, *S(f)* is the source excitation function, *R(f, q)* is the source radiation pattern, *G(d)* is the *Lg* geometrical spreading function, *I(f)* is the instrument response, *SS(f)* is the station site response, *G(f, q)* is anelastic attenuation function which can be written by

$$G(f, q) = e^{-\gamma d} \quad (2)$$

where γ is the attenuation coefficient, which is related to the quality factor Q and the group velocity U as

$$\gamma = (pf)/(QU). \quad (3)$$

Assuming two events lie within a few degrees of the great-circle path connecting the receiver and the two epicenters, we obtain the ratio of *Lg* wave spectral amplitude for event 2 (the distant event) to that for event 1 (the nearer event) as

$$A(f, d_2)/A(f, d_1) = [S_2(f)/S_1(f)][G(d_2)/G(d_1)]\exp[-\gamma\Delta], \quad (4)$$

Where the indices 1 and 2 represent event 1 and event 2, respectively, and Δ is the distance between the two events. Note that the source radiation pattern $R(f, \theta)$ does not show up in (4) because source radiation and is assumed to be azimuthally independent to first order in *Lg* signals (Sereno, 1990; Shih et al., 1994). The site amplification term canvels out for small difference in back azimuth. For geometrical spreading function *G(d)*, we adopted $G(d) = d^{-0.5}$ for *Lg* wave in the frequency domain (Shin and Herrmann, 1987). To solve for the attenuation coefficient , we need to estimate the effects of the source excitation term *S(f)*, which can be represented by the ω^{-2} model as

$$S(f) = S_0/(1+f^2/f_c^2), \quad (5)$$

where S_o is a constant for a given event, and f_c is the corner frequency. The corner frequency f_c is related to the stress drop, $\Delta\sigma$, the shear wave velocity at the source, υ_β, and the seismic moment of the event, M_0 (Brune, 1970). If the difference in f_c for the two events is small, then, as a first order approximation, (5) can be simply reduced to $S(f) \cong S_0$. One can assume constant stress drop and scale corner frequency with moment, but this is rather arbitrary given observed scatter in measured stress drops. Since our spectral ratios are bandwidth limited by low *Q* values, we ignore small high frequency corrections and restrict our analysis to frequencies below 0.5-1.0 Hz. Thus, we can rewrite (4) as

$$A(f, d_2)/A(f, d_1) = [S_{02}/S_{01}][d_2/d_1]^{-0.5}\exp[-\gamma\Delta], \quad (6)$$

and solve for the attenuation coefficient $\gamma(f)$. Our simplified source correction is approximately equivalent to shifting the spectral ratio to a zero base line for its low-frequency limit. We found that use of the seismic moments from the Harvard CMT solutions provided spectral ratios with small scatter for different event pairs with about the same magnitudes. Because not all of the events studied have Harvard CMT solutions available, we first constructed a reference spectral ratio curve by averaging all spectral ratios after source corrections. Other spectral ratios were shifted relative to the reference spectral ratio by correlating over the frequency band of 0.2-0.5 Hz. Finally, a stacked average is calculated from all spectral ratios for all event pairs to provide a representative *Lg* attenuation, $\gamma(f)$, along a profile.

We constructed four profiles approximately in the north-south direction. Figure 4 shows the locations of selected events used for estimating *Lg* attenuation. The first three profile are positioned in the western, central, and eastern parts of the Tibetan Plateau, respectively, with events near the southern and northern margins and the associated paths crossing the Plateau. The fourth profile covers a relatively small area in the central part of northern Tibet, where strong *Lg* attenuation was observed. In order to approximate great circle paths, only events with back azimuths within 30 degrees are used in calculating $\gamma(f)$. The number of events used for each profile is 4x3, 7x8, 4x7, and 5x6, respectively, where the first number represents the number of events in the north and the second is the number of events in the south. The reference *Lg* attenuation curves were usually the average of many event pairs. 15 event pairs were used for profiles II and III, and 8 event pairs for profile IV. For profile I, the reference *Lg* attenuation curve was calculated using only three event pairs, and is less reliable. The spectral ratios are calculated out only to 1 Hz, given the low signal-to-noise ratio at higher frequencies.

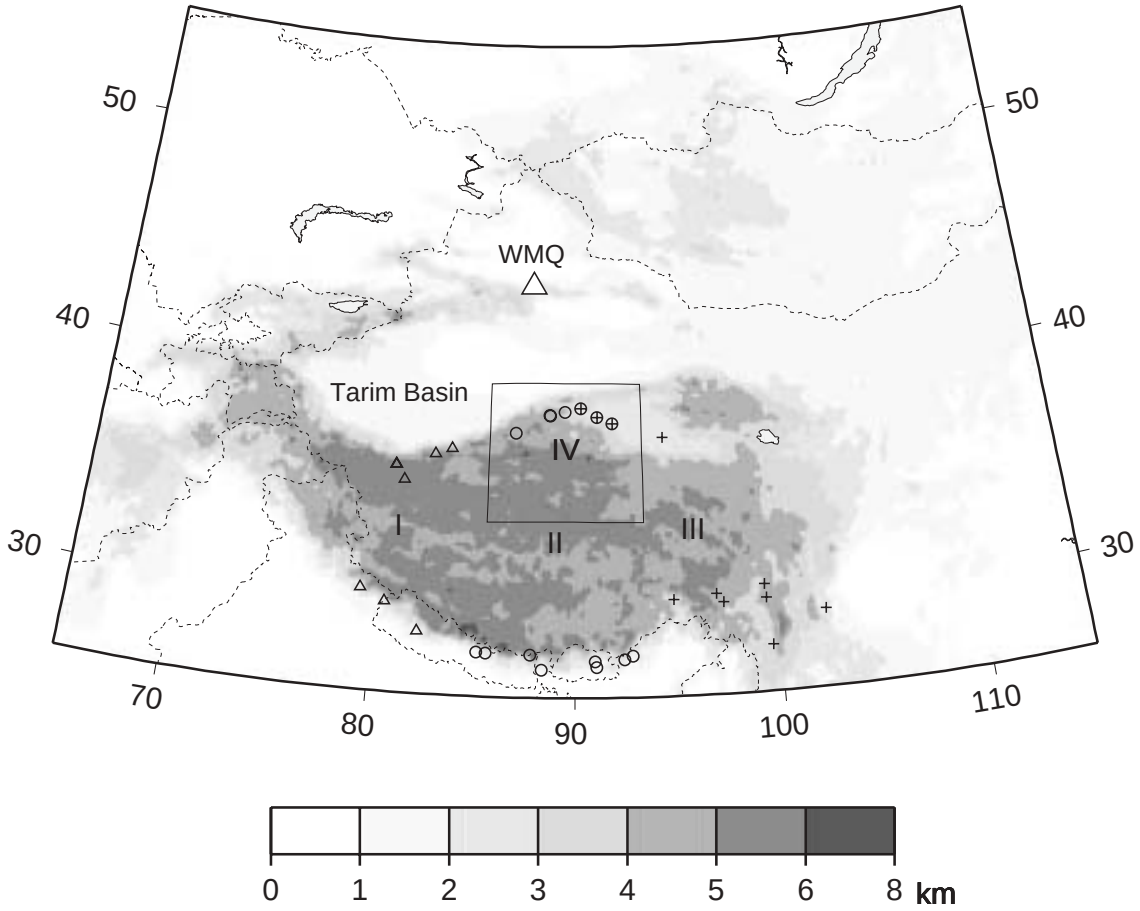

Figure 4. Map indicating the corridors for which 2-station estimates of Lg attenuation are made. The events are either on the northern or southern margin of the Plateau, or for the case of corridor IV, the northern and central Plateau.

The *Lg* attenuation coefficients γ(f) for each profile show clear frequency dependence across the band of 0.1-1.0 Hz. Scatter in the 0.2-0.5 Hz band was minimized by our processing. The largest scatter is observed for profile IV. In general, the *Lg* attenuation γ(f) increases with frequency up to about 1Hz for profiles I, II, and III and up to about 2 Hz for profile IV, then it gradually drops off. This drop off may be caused in part by lack of high frequency source corrections, but mainly is due to high frequency *Sn* coda in the *Lg* window at large distances. The rate of increase in *Lg* attenuation γ(f) is not a constant function of frequency and differs for each profile. The highest attenuation and the best linearity for LOG[γ(f)] of *Lg* are observed in profile IV, where rapid attenuation is observed across a short distance range.

Assuming a power-law frequency dependent model, *Lg* attenuation can be written in terms of quality factor Q_{Lg} as

$$Q_{Lg}(f) = Q_0 f^{\eta}, \qquad (7)$$

where Q_0 is the value of Q_{Lg} at 1 Hz, and η is the power-law frequency dependence. Based on equations (3) and (7), we fit a Q_{Lg}(f) model to observed γ(f) to estimate the value of *Lg* attenuation in various areas of the Tibetan Plateau. The logarithmic *Lg* attenuation coefficients γ(f) are fit to a Q_{Lg}(f) model by least-squares linear regression in two frequency bands, 0.2-0.5 Hz and 0.2-1.0 Hz, for each profile. Figures 5a-d show our results. The numerical values of the best-fit model parameters *Lg* Q_0 and η are listed in Table 1. Previous research on *Lg* attenuation in Asia indicates that η is very sensitive to lateral heterogeneity in the

Table 1. The values of *Lg* attenuation in different parts of Tibet.

		Profile I	Profile II	Profile III	Profile IV
0.2-0.5 Hz	Q_o	146±20	149±14	122±20	90±10
	η	0.67±0.12	0.20±0.09	-0.19±0.15	0.15±0.10
0.2-1.0 Hz	Q_o	160±5	224±9	195±14	85±2
	η	0.75±0.04	0.58±0.06	0.24±0.08	0.10±0.04

crust, thus reliable η estimates are difficult to obtain [Shih et. al., 1994], so we limit our discussion mainly to the quality factor Q_0.

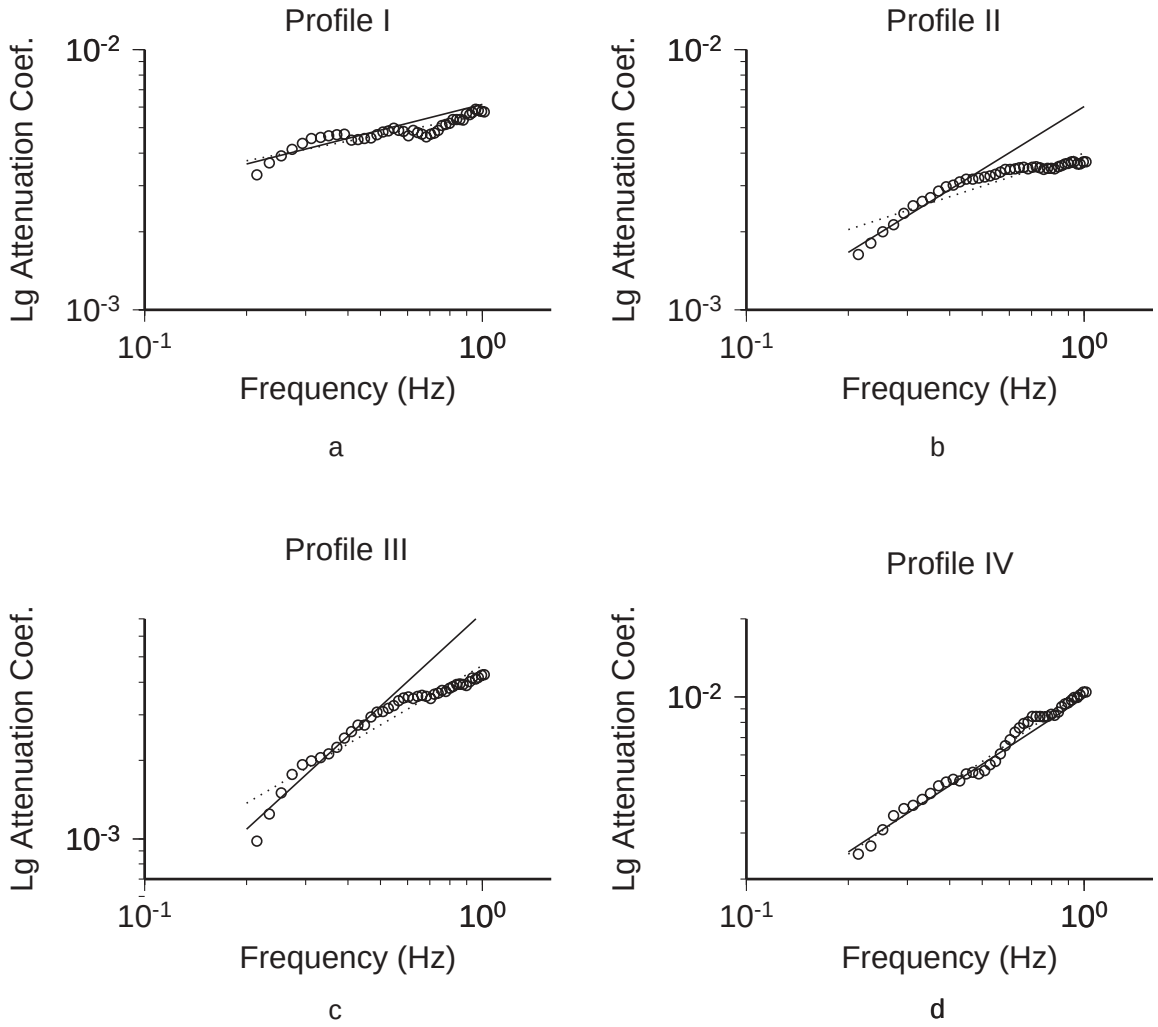

Figure 5. Lg attenuation coefficient *g(f)* and the best fit Q_{Lg} models (straight lines) for each profile. Circles are mean values estimated from stacking multiple spectral ratios in each profile. Solid and dashed lines represent the best fit Q_{Lg} models in frequency bands of 0.2-0.5 Hz and 0.2-1.0 Hz, respectively.

We found that Q_0 values differ for each profile. There is little difference in Q_0 for profile IV between the two best-fit models because the logarithmic spectra are very linear. However, there are variations in the Q_0 estimates for the other profiles between the 0.2-0.5 Hz and 0.2-1.0 Hz bands. Profiles II and III show a reduced slope in logarithmic γ(f) commencing at about 0.5 Hz. Thus, broader band estimates give higher Q_0 values. We believe that this is likely due to contamination at higher frequencies (above 0.5 Hz) by increased contribution of high frequency *Sn* coda rather than true *Lg* signals. The Q_0 value of *Lg* for the Tibetan Plateau as a whole is in a

range of about 120-150 for the 0.2-0.5 Hz band, and in a range of 160-230 for the 0.2-1.0 Hz band based on the results for profiles I, II and III. Our observations indicate that a region in northern central Tibet close to the Plateau margin is characterized by very strong *Lg* attenuation, with a Q_0 value of 85-90. This is consistent with observed high frequency amplitude decay by a factor of ten or more in that region (see Figure 2).

CONCLUSIONS AND RECOMMENDATIONS

The Tibetan Plateau appears to have very strong attenuation of *Lg* phases for paths within and traversing the northern boundary of the Plateau. This is demonstrated by the broadband spectral behavior of *Lg*, which undergoes a systematic shift of apparent corner frequency from 2 to 0.2 Hz as a function of path length. The *Lg* attenuation estimates obtained here are much lower than those in the literature, most of which are for eastern Tibet. Recently, Xie (2001) has reanalyzed the *Lg* spectra data used by McNamara et al. (1996), obtaining a Q_{Lg} model with $Q_0 = (126\pm9)$ and $\eta = (0.37\pm0.02)$, which is very consistent with our estimates in profiles II and III, where the data overlap. Xie s estimate is for the 0.2-3.6 Hz band, with the extension to higher frequency being viable due to the short path lengths involved. This extrapolates smoothly up from our 0.2-0.5 Hz band prior to the decrease in slope of LOG[γ(f)]. Phillips et al. (2000) obtain tomographic models of Q_{Lg} with values of 200 in Tibet south of the Qaidam and Tarim basins. Their results give $Q = 500$ for the Tarim Basin, compatible with our observation of efficient propagation there. Their coverage of western Tibet is very limited due to constraining the data to 0.75-1.5 Hz, which is strongly attenuated over longer paths in Tibet.

We resolve a region in northernmost Tibet with much lower Q than previously reported by any study of Tibet. Figure 6 summarizes our Q estimates, illustrating the localized region with Q values of 85-90. Profile II gives overall Q values of 149 for the 0.2-0.5 Hz band, which requires that Q increase in southern central Tibet to a value of 265 or higher for a northern Q of 90. Phillips et al. (2000) also indicate such an increase in Q from north to south, but they have high values approaching 500 near LSA, which is consistent with Q value of 85 in the northern part of Tibet.

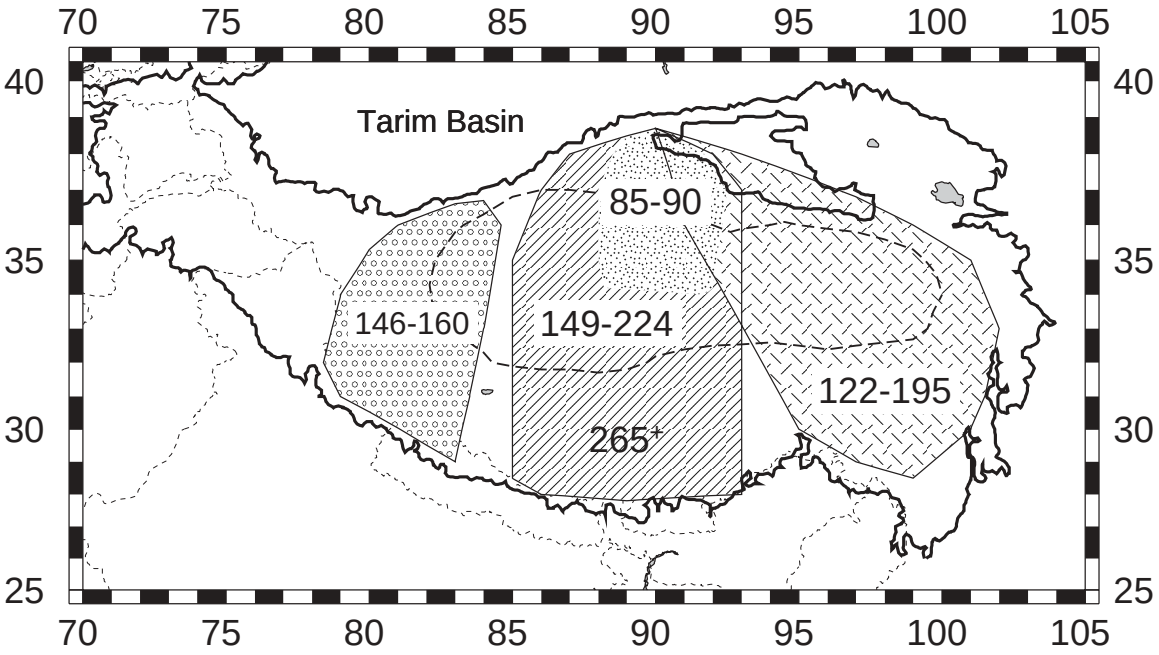

Figure 6. Summary map indicating Qo values for different corridors. The lower values are preferred.

Our values of Q_{Lg} of 100-200 are found in other tectonically active areas, such as California (Herrman, 1980; Nuttli, 1986) and Iran (Nuttli, 1980). In general, the mechanisms of intrinsic attenuation are very sensitive to temperature conditions, and the very low Q_{Lg} of 85-90 may be associated with partial melting in northern Tibet. Owens and Zandt (1997) presented evidence for a lower crustal low-velocity zone likely to involve partial melt

in northern Tibet. This region has inefficient *Sn* propagation (Ni and Barazangi, 1983; McNamara et al., 1995), low *Pn* velocity (McNamara et al., 1997), and high Poisson s ratios of 0.34-0.35 over a 30 km thickness (Owens and Zandt, 1997). Figure 7 shows a north-south profile through Tibet adapted from Owens and Zandt (1997), indicating the coincidence of the partial melt zone in the deep

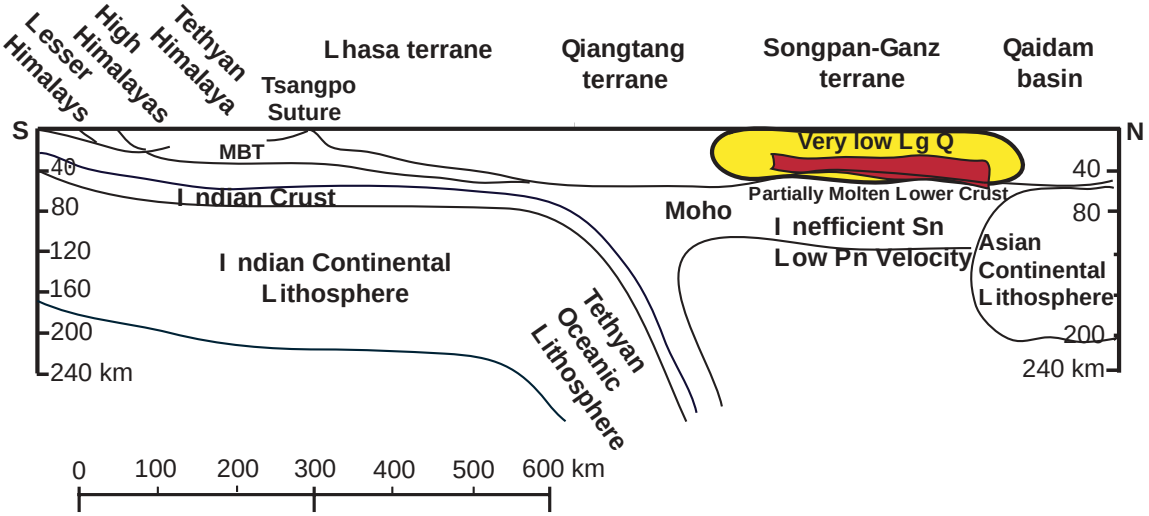

Figure 7. Cross-section through Tibet indicating the coincidence of the region of very low Q_{Lg} and partial melt in the crust, as well as Sn inefficiency and low Pn Velocity.

crust of northern Tibet and the region of low *Lg Q*. Further analysis is required to constrain the spatial extent of the very low *Q* region affecting *Lg*, but it is clear that Tibet can not be viewed as a region with uniform *Lg* attenuation, nor as a region with extensive *Lg* attenuation values in the range of 340-450 as previously indicated. There is some evidence for partial melt and crustal low-velocity zones existing north of the Tsangpo suture in southern Tibet (Nelson et al., 1996; Kind et al., 1996; Cotte et al., 1999). This low-velocity zone may also relate to a localized low Q_{Lg} region, however, it is not yet resolved by our data set due to lack of resolution in southern Tibet.

REFERENCES

Brune, J. N. (1970), Tectonic stress and the spectra of seismic shear waves from earthquake sources, *J. Geophys. Res., 84*, 2262-2272.

Cotte, N., H. Pedersen, M. Campillo, J. Mars, J.F. Ni, R. Kind, E. Sandvol., and W. Zhao (1999), Determination of the crustal structure in southern Tibet by dispersion and amplitude analysis of Rayleigh waves, *Geophys. J. Int*., *138*, 809-819.

Herrmann, R. B. (1980), Q estimates using the coda of local earthquakes, *Bull. Seism. Soc. Am*., *70*, 447-468.

Kind, R., et al. (1996), Evidence from earthquake data for a partially molten crustal layer in southern Tibet, *Science*, *274*, 1652-1654.

McNamara, T. J. Owens, and W. R. Walter (1995), Observations of regional phase propagation across the Tibetan Plateau, *J. Geophys. Res., 100*, 22215-22229.

McNamara, W. R. Walter, T. J. Owens, and C. J. Ammon (1997), Upper mantle velocity structure beneath the Tibetan Plateau from Pn travel time tomography, *J. Geophys. Res., 102*, 493-505.

McNamara, D. E., T. J. Owens, and W. R. Walter (1996), Propagation characteristics of L_g across the Tibetan plateau, *Bull. Seism. Soc. Am*., *86*, 457-469.

Nelson, K. D., et al. (1996), Partially molten middle crust beneath southern Tibet: Synthesis of project INDEPTH results, *Science*, *274*, 1684-1688.

Ni, J. and M. Barazangi (1983), High-frequency seismic wave propagation beneath the Indian Shield, Himalayan Arc, Tibetan Plateau and surrounding regions: high uppermost mantle velocities and efficient S_n propagation beneath Tibet, *Geophys. J. R. astr. Soc.*, *72*, 665-689.

Nuttli, O. W. (1980), The excitation and attenuation of crustal seismic phases in Iran, *Bull. Seism. Soc. Am*., *70*, 469-485.

Nuttli, O. W. (1986), Yield estimates of Nevada test site explosions obtained from seismic *Lg* waves, *J. Geophys. Res., 91*, 2137-2152.

Owens, T. J. and G. Zandt (1997), Implications of crustal property variations for models of Tibetan plateau evolution, *Nature, 387*, 37-43.

Phillips, W. S., H. E. Hartse, S. R. Taylor, and G. E. Randall (2000), 1 Hz *Lg* Q tomography in central Asia, *Geophys. Res. Let*., *27*, 3425-3428.

Rapine, R. R., J. F. Ni, and T. M. Hearn (1997), Regional wave propagation in China and its surrounding regions, *Bull. Seism. Soc. Am*., *87*, 1622-1636.

Reese, C. C., Rapine, R. R., and J. F. Ni (1999), Lateral variation of Pn and Lg attenuation at the CDSN station LSA, *Bull. Seism. Soc. Am*., *89*, 325-330.

Ruzaikin, A. I., L. Nersesov, V. I. Khalturin, and P. Molnar (1977), Propagation of *Lg* and lateral variations in crustal structure in Asia, *J. Geophys. Res*., *82*, 307-316.

Sereno, T.J., S. Bratt, and T. Bache (1990), Frequency-dependent attenuation in eastern Kazakhstan and implications for seismic detection thresholds in the Soviet Union, *Bull. Seism. Soc. Am*., *80*, 2089-2105.

Shih, X. R., K.-Y. Chun, and T. Zhu (1994), Attenuation of 1-6 s *Lg* waves in Eurasia, *J. Geophys. Res*., *99*, 23859-23874.

Shin, T.-C. and R. B. Herrmann (1987), *Lg* attenuation and source studies using 1982 Miramichi data, *Bull. Seism. Soc. Am*., *77*, 384-397.

Xie, J. (2001), *Lg* Q in the Eastern Tibetan Plateau, submitted to *Bull. Seism. Soc. Am*.